Characteristics of correlation satellites below 25 eV in xenon probed by pulsed-field-ionization–zero-kinetic-energy photoelectron spectroscopy

R. C. Shiell,[1] M. Evans,[2] S. Stimson,[2] C.-W. Hsu,[3] C. Y. Ng,[2] and J. W. Hepburn[1]
[1]*Chemistry Department, University of Waterloo, Waterloo, Ontario, Canada N2L 3G1*
[2]*Department of Chemistry, Iowa State University, Ames, Iowa 50011*
[3]*Chemical Science Division, Lawrence Berkeley National Laboratory, Berkeley, California 94720*
(Received 10 September 1998; revised manuscript received 12 November 1998)

The technique of pulsed-field-ionization–zero-kinetic-energy photoelectron spectroscopy, typically applied to the investigation of ionic states of atoms and molecules resulting from single electron excitation, has been used to probe all known correlation ionic states of xenon up to 25 eV. The high-resolution (1 meV) spectra that result show the formation of satellite states clearly resolved from their neighbors. Their intensities are comparable to that of the $5s5p^6\ ^2S_{1/2}$ main line ionic state and for a given multiplet are relatively independent of the total angular momentum of the ionic state formed. The Rydberg states converging onto different ionic limits demonstrate effective lifetimes that are related to the excitation of the associated ionic core. These spectra allow the determination of relative intensities, and from them, the partial cross sections for the formation of each state at threshold. This supplements the existing intensity studies from the near-threshold to the x-ray region and increases our understanding of the dominant correlation processes within this atom as a function of photon energy. [S1050-2947(99)04804-0]

PACS number(s): 32.80.Rm, 33.80.Rv, 32.80.Fb

I. INTRODUCTION

Probing the formation and characteristics of ionic states within atoms and molecules is the primary aim of photoelectron spectroscopy. Above the lowest ionization energy of these species irradiation with light can result in the formation of single-hole ionic states with the ejection of one electron (a ''main line'' peak in a photoelectron spectrum) or ''satellite'' ionic states in which one electron is ejected and a second excited from the neutral configuration. Each of these ionic thresholds has a series of neutral singly excited or doubly excited Rydberg states converging onto them, respectively, and these may decay to lower-lying ionic states through the process of autoionization. The observation of main line peaks in photoelectron spectra or the neutral states associated with them may be understood by invoking the single-particle model while formation of the remaining states is forbidden within this approximation and is solely the result of the correlated motions of electrons within the species. The propensity for formation of each ionic state as a function of photon energy reflects the change in the dominant correlations and it is therefore useful to compare sets of such data at different photon energies.

In order to obtain partial cross sections at threshold using photoelectron spectroscopy, static electric fields are traditionally employed to allow the selective detection of those electrons formed with near-zero kinetic energy as the photon energy is scanned over the thresholds for formation of each cationic state [1]. Satellite states can be difficult to probe using this technique; in general such states are formed at high photon energies, they produce low signal intensities, and they contribute to a highly congested spectrum. Further, in order to discriminate against the observation of those states formed through nearby autoionizing resonances that result in low kinetic energy electrons there is a need for a high degree of rejection of such electrons, and the effectiveness with which this is accomplished depends upon the electron optical properties of the analyzer, lenses, and electrode surfaces. The separation between high-energy and threshold contributions to the observed signal at each ionic threshold can be difficult to achieve, and requires a highly selective experimental technique. The introduction of pulsed-field-ionization–zero-kinetic-energy (PFI-ZEKE) photoelectron spectroscopy in recent years [2] has largely overcome this problem and enabled a high-resolution spectroscopic probe of ionic states formed by excitation and subsequent field ionization.

PFI-ZEKE photoelectron spectroscopy exploits the long lifetimes of high-n Rydberg states converging to each ionic threshold in a species. With the use of a pulsed light source these long lifetimes enable the selective detection of electric-field ionized electrons from these states while maintaining successful discrimination against prompt electrons released in conjunction with the formation of lower-lying ionic states. A schematic of this process is displayed in Fig. 1, where the excitation energy is scanned across two ionization thresholds, $|1\rangle$ and $|2\rangle$, and the resulting peaks in the spectrum correspond to pulsed excitation and subsequent field ionization of the manifold of high-lying Rydberg states below each threshold. This technique has the added advantage that it can probe the lifetimes of Rydberg states converging upon each ionic limit by changing the delay between the light excitation and field ionizing pulses and subsequent comparison of recorded intensities [3,4]. In conjunction with laser sources with light pulses repeated every several milliseconds or more, a delay between the excitation light pulse and the ionization electric-field pulse of typically a few μs is used, resulting in selective observation of the cation state of interest. With such light sources, the practical energy range is limited

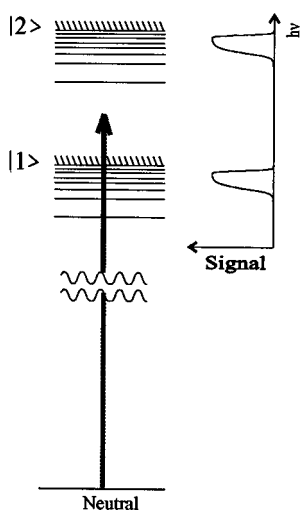

FIG. 1. A schematic illustration of the PFI-ZEKE process. As the incident photon energy is scanned across each ionic limit, to which Rydberg series converge, a manifold of these high Rydberg (long-lived) states can be formed, which may then be field ionized. The resulting electrons are selectively detected with effective discrimination against any electrons released in conjunction with the formation of lower-lying ionic states.

up to just above 19 eV [5,6] and thus only the formation of cations in their lower electronic states is detected. A spectrometer at BESSY has recently been developed with which the formation of satellite states in nitrogen from 23–26 eV [7] and argon from 41–45 eV [8] with resolutions of 10 and 40 meV, respectively, have been detected using pulsed fields. We have previously reported the use of a high-resolution spectrometer at the Chemical Dynamics Beamline [9] at the Advanced Light Source (ALS) to detect the 5*s* main line state and seven satellite states of xenon and obtain their relative intensities for formation with a precision of ≈25% [10]. The present results show these ionic states formed with several orders of magnitude improved signal to noise ratio, extend these measurements to include three states not previously observed below 25 eV and demonstrate, through modifying the delay between excitation and field ionization, effective lifetimes of the Rydberg manifolds below each ionic limit that are dependent upon the state of the ionic core.

The xenon satellite spectrum has been measured over a wide incident photon energy range from the near-threshold [11] to the x-ray [12] regions and the partial strengths of various ionic states have been obtained. The resolution with which low-lying satellite states have been observed is typically 50 meV at photon energies of 40.8 eV [13], 130 meV at energies less than 100 eV [14], and 300 meV at 1.487 keV [12]. In the region containing the lowest-lying satellite states of xenon 10 ionic states are known to exist from 23.6–25.0 eV, with some separated by an energy as small as 5 meV [15]. Obtaining the partial cross sections of each ionic state at any photon energy is therefore often complicated by the fact that there are many unresolved satellite states belonging to different symmetry manifolds within the spectrum and it is for this reason that at threshold the high-resolution PFI-ZEKE technique is particularly suited to the study of these states.

II. EXPERIMENTAL DETAILS

The spectrometer has been discussed in detail elsewhere [9] and so only an outline will be given here. An atomic beam of 99.999% (research grade) xenon effused through a metal nozzle of 0.5 mm diameter at 298 K and intersected the photon beam 0.5 cm from the nozzle. This resulted in an increase in the number density of atoms in the interaction region compared to that of our previous study [10] by two orders of magnitude, with a concomitant increase in resulting signal to noise ratio for each peak. The interaction volume, lying between two electrodes across which the ionizing electric pulse was applied, formed the center of the acceptance region of a tandem steradiancy-hemispherical analyzer. This region presented an estimated active area of 7.1 mm^2 to the analyzer system, with the result that atoms drifted out of the detection volume in ≈6 μs.

The ALS was operated in multibunch mode, with 272 light micropulses (separated by 2 ns), one dark gap of length 81 ns, one additional light micropulse, and a 33-ns dark gap all within one ring period (656 ns). As the photon energy was scanned across high-lying states that converge to an ionic state, Rydberg states of xenon containing one highly excited electron were formed. Below the threshold for the $5s^{-1}$ state at 23.397 eV these Rydberg states were singly excited and below each threshold for satellite formation (e.g., the $5s^2 5p^4(^3P)6s\ ^4P_{5/2}$ ion state at 23.669 eV) they were doubly excited states with one electron in a high-*n* state. During the 80-ns dark gap a 40-ns pulsed electric field of 0.67 V/cm was applied to the interaction region, field ionizing those states lying within ≈4 cm^{-1} (0.5 meV) of an ionic limit [16], and accelerating the resulting near-threshold electrons towards the analyzer for selective detection. The resulting spectrum shows the (unresolved) manifold of high Rydberg states converging towards each (resolved) ionic limit, with the intensity of each peak reflecting state-dependent excitation and decay probabilities.

The photon energy was scanned across the 5*s* main line state and nine of its correlation satellite states from 23.6–24.9 eV in steps of 0.5 meV with a photon bandpass of 1.5 meV. Once detected, each individual line was repeatedly sampled with steps of 0.2 meV and a photon bandpass of 0.7 meV. By calibrating the photon energy scale using the ionization onsets of neon and helium, the positions of the lines were found to be at their expected positions within experimental uncertainty (≈0.5 meV). A more exact energy calibration was done by comparison with the known optical data [15].

The timing structure of the experiment was modified to investigate the effective lifetimes of the Rydberg states that converge to the different ionic limits in xenon. Below each threshold, at a particular photon energy, the number of Rydberg states formed during each period due to the 273 micropulses of light is assumed to be constant for all periods. A comparison of the intensity of the signals obtained when the pulsed electric field is applied after various numbers of ring periods provides an effective lifetime for each manifold of Rydberg states. With the electric field pulse applied every ring period a signal is observed that reflects the formation

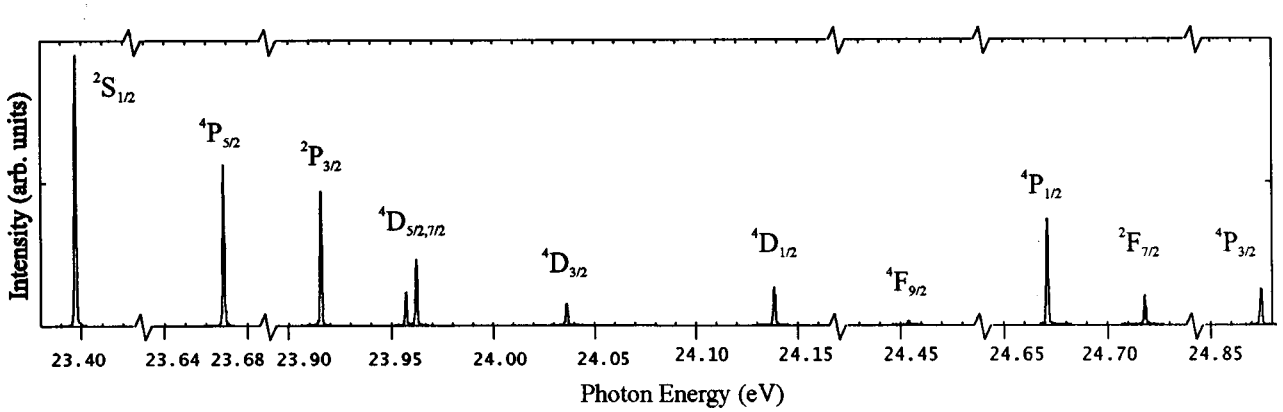

FIG. 2. A split-energy spectrum with consistent energy scale, normalized by photon flux, of the ionic states in xenon observed through PFI-ZEKE photoelectron spectroscopy, with the pulsed field applied once every synchrotron period. The main line state at 23.397 eV is shown and ten correlation satellites. The position of each peak is calibrated from the analysis by Hansen and Persson [15] and labeled with *LS* notation, see text.

and decrease in the number of detectable Rydberg states in the time up to 616 ns before the 40-ns pulse. Conversely, with the electric field pulse applied every three periods a signal is obtained that is dependent upon the formation and decrease in number of states up to 1.928 μs before this pulse. In both cases the total light flux, and therefore the number of Rydberg states created per second, is the same. The difference between the observed signals is therefore caused by the decrease in the number of Rydberg states in the detection volume due to both their finite lifetime and the original drift velocity of the atomic beam. Scans were taken across each of the ionic state thresholds in xenon with the pulsed field applied every 1 and 3 periods. Under the assumption that each manifold of Rydberg states converging to an ionic limit can be modeled by a single effective lifetime τ, these were determined by a similar method to that used in Ref. [17], and described below.

When the electric field pulse is applied once every ring period, the number of Rydberg states detected per second (i.e., those that are created and survive until the application of each electric field pulse) may be written as $I(1)$. Similarly the number of counts per second when the electric field pulse is applied every three periods reflects the possible decay of the Rydberg states during either the first or second ring periods and is given by

$$I(3)=\frac{I(1)}{3}(1+e^{-t_p/\tau}+e^{-2t_p/\tau}), \tag{1}$$

where t_p is the time period of the ring (656 ns). The ratio of the signals, $I(1)/I(3)$, allows a calculation of the effective lifetime τ for the Rydberg states converging to each ionic limit, within the approximation that the decay may be represented by one constant.

For those signals that demonstrated an effective lifetime of >6 μs by which time the original drift velocity of the atoms is expected to dominate the loss in signal, no value of effective lifetime is recorded. As can be seen below, a considerable range of lifetimes was nonetheless observed for different ionic states to which the Rydberg series converged.

III. RESULTS

Figure 2 shows a split energy scale spectrum of the observed ionic states formed due to PFI-ZEKE in xenon. Within the energy range sampled the 5*s* main line peak (the $5s5p^6\ ^2S_{1/2}$ state) and the ten known satellite peaks were easily resolved. In our previous study we attempted to observe, but did not detect, the $5s^25p^45d\ ^4F_{9/2}$ state [10] and concluded that its intensity was less than that of the $5s^25p^45d\ ^4D_J$ states; this is confirmed by the present work. Additionally, we observe the $5s^25p^45d\ ^2F_{7/2}$ and the $5s^25p^46s\ ^4P_{3/2}$ ionic states formed through the PFI-ZEKE process. The states are labeled with the more familiar *LS* designations although it is noted that one could alternatively use *jK* designations. Hansen and Persson have calculated the purity of these ionic states under both coupling schemes [15] and the average purities do not differ significantly.

An expanded view of the observed $5s^25p^45d\ ^4D_{5/2}$ and $^4D_{7/2}$ states with the pulsed field applied every one, two, three, and five ring periods is given in Fig. 3, and each spectrum, with a consistent intensity scale, shifted vertically for clarity. These spectra demonstrate a full width at half-maximum (FWHM) of 0.9 meV and show the shorter effective lifetime of those Rydberg states converging to the $^4D_{7/2}$ state relative to those associated with the $^4D_{5/2}$ state. The intensities of all peaks were calculated by computing the areas under the peaks after subtraction of the background level. Values for the effective lifetimes were calculated as described above by a comparison of $I(1)$ and $I(3)$, and the absolute value recorded in Table I if they were less than 6 μs. Those states that showed a negligible decrease in intensity (less than 10%) between the electric pulse being applied every one and three ring periods were labeled with a lifetime of >6 μs. The relative intensities at threshold for each ion state were then found by extrapolating the decay curve to zero time and displayed in Table I relative to that of the 5*s* main line state with magnitude 100. The experimental error in each calculated intensity, due to variations in conditions and statistical fluctuations, is estimated to be approximately 5%, and slightly more for the less intense peaks. For comparison the reported relative peak heights of these satellite states formed from unpolarized He II α light at 40.8 eV [13]

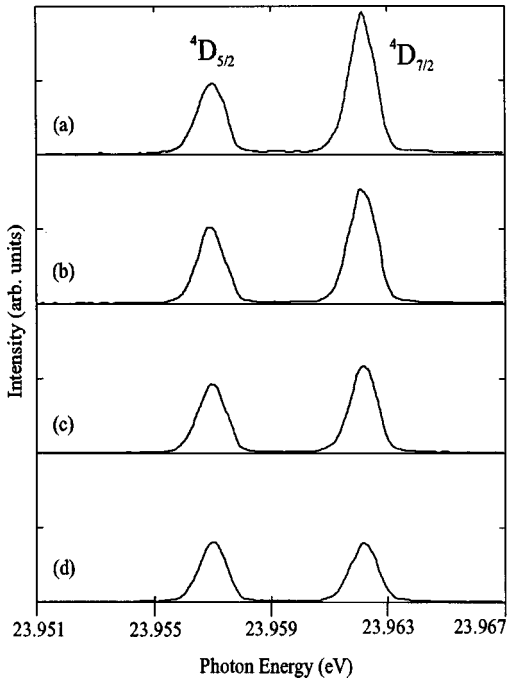

FIG. 3. An expanded view of the observed $5s^25p^45d\ ^4D_{5/2}$ and $^4D_{7/2}$ states with the pulsed field applied every (a) one, (b) two, (c) three, and (d) five ring periods (one ring period is 656 ns). These spectra demonstrate a full width at half-maximum (FWHM) of 0.9 meV and show the shorter effective lifetime of those Rydberg states converging to the higher ionic threshold. The spectra have consistent intensity scale and have been shifted vertically for clarity.

and polarized synchrotron light at 63.5 eV [18] are shown in Table I. It should be noted that the former is not taken at the magic angle with respect to the beam (see [14] for details) and thus could show a maximum difference by a factor of four from the true relative cross sections of some states. The asymmetry parameter of the $5s^{-1}$ peak has been well studied and is observed to have a β of $\approx$1.8 at 40.8 eV approaching a value of 2 at higher energies [1], as expected by a nonrelativistic single-electron model. At 72 eV the asymmetry parameter for the $5s^25p^46s\ ^2P_{3/2}$ state is known to be strongly negative and for the $5s^25p^46s\ ^4P_{1/2}$ state to be 1.98, but little else is known about the angular distributions of electrons after formation of these states at incident photon energies below 30 eV or the other ionic states in this region [14]. Inclusion of configuration interaction with the $5s5p^6\ ^2S_{1/2}$ ionic state results in $\beta\rightarrow 2$, although mixing with other states tends to reduce this value [19].

Also shown in Table I are the absolute partial ionization cross sections of the satellites, calculated from our intensity data. These were obtained by scaling the 5*s* photoionization cross-section data of Samson and Gardner [20], which were recorded at photon energies down to 23.55 eV and show a leveling off towards threshold of 0.5 Mb. A recent theoretical and high-resolution experimental study of the fluorescence from the $5s5p^6\ ^2S_{1/2}$ ionic state by Schmoranzer *et al.* [21], scaled to the cross section of Samson and Gardner at 23.74 eV, demonstrates several resonances within this region, but does indicate the validity of using the 0.5-Mb value for direct ionization at threshold.

IV. DISCUSSION

A. Cross sections at threshold

In order to understand correlation effects within multielectron species, they are addressed by either of two formally equivalent methods: configuration interaction (CI) or many-body perturbation theory (MBPT). To a first approximation the dominant processes can be separated into ''intrinsic,'' those that exist in the absence of a photon, or ''dynamic,'' which show a significant dependence upon the kinetic energy of the outgoing electron [22]. The former include ground- and final-state correlations and are included within the CI

TABLE I. Characteristics of Rydberg states converging towards 11 of the ionic states of xenon with binding energies below 25 eV observed at their respective thresholds, at 40.8 and 63.5 eV.

Ion state[a]	Energy (eV) (Ref. [15])	Lifetime (μs) (this work)	Relative Intensities[b]			Cross section at threshold[d] (Mb)
			At threshold (this work)	At 40.8 eV[c] (Ref. [13])	At 63.5 eV (Ref. [18])	
$5s5p^6(^2S_{1/2})$	23.3967	>6	100	100	100	0.50
$(^3P)6s(^4P_{5/2})$	23.6689	>6	60	0.21		0.30
$(^3P)6s(^2P_{3/2})$	23.9164	>6	55	0.76	0.2	0.28
$(^3P)5d(^4D_{5/2})$	23.9576	>6	15	0.52		0.08
$(^3P)5d(^4D_{7/2})$	23.9627	1.2	22	0.09		0.11
$(^3P)5d(^4D_{3/2})$	24.0366	4	9.4	0.58		0.05
$(^3P)5d(^4D_{1/2})$	24.1388	2.3	13	0.23		0.06
$(^3P)5d(^4F_{9/2})$	24.4546	0.8	3.1	0.74	0.2	0.02
$(^3P)6s(^4P_{1/2})$	24.6719	>6	45	2.4	4.8	0.23
$(^3P)5d(^2F_{7/2})$	24.7188	1.2	9.6	1.4		0.05
$(^3P)6s(^4P_{3/2})$	24.8754	>6	16	0.43	0.1	0.08

[a]States given in *LS* notation. The parental configuration of the satellite states is $5s^25p^4(^3P)$.

[b]The intensity for the $5s^{-1}$ main line is arbitrarily normalized to 100.

[c]Data not taken at the magic angle, see text.

[d]Scaled from the data for threshold formation of the $5s^{-1}$ state from Samson and Gardner, Ref. [20].

model by initial and final ionic state configuration interaction (ISCI and FISCI) calculations. The dynamic correlation effects may be modeled by the inclusion of continuum state configuration interaction, or more generally interchannel coupling, within the CI picture, corresponding to relaxation or shake up, conjugate shake up and inelastic scattering within the MBPT calculation. Generally all of the possible effects will be present but the dominant ones change with photon energy: e.g., shake up dominates at high kinetic energy and inelastic scattering shows an enhancement near threshold.

The results that are reported above reflect either single or double excitation to a Rydberg state and subsequent removal of the Rydberg electron by the pulsed electric field. Due to the continuity of oscillator strength the cross section per unit energy for excitation and subsequent removal of the outer electron below threshold is expected to develop smoothly into the partial ionization cross section above threshold. If there is no resonant enhancement of the initial (singly excited at 23.397 eV and doubly excited at the other energies) Rydberg states, then the relative intensities of the PFI-ZEKE peaks with a specific time delay between light excitation and field ionization will reflect the relative partial cross sections for *direct* formation of the corresponding ionic states at threshold together with any state dependent decay or stabilization mechanisms. The thresholds for the satellite states are at least 20 meV from known resonances and equally distributed between sharp and diffuse resonances [23]. For the case of the $^2S_{1/2}$ main line state, however, there is an observed unassigned resonance 1 meV below the $5s^{-1}$ ionic state (line 61 in [23]) and an assigned $(^3P)5d\ ^4D_{1/2}8p_{3/2}$ doubly excited resonance 3 meV above this state [21]. In the PFI-ZEKE spectrum at 23.397 eV we observe no second peak corresponding to the detection of energetic electrons from the decay of either resonance, but cannot state with certainty that they do not make a contribution to the absolute partial cross section for formation of this state. The photoion yield curve obtained over the energy range of the satellite states shows a steady decrease and little variation at the thresholds for each ionic state [24], implying little resonant contribution to the displayed cross-sections.

From Table I it is apparent that satellite states with high- and low-J values are formed at threshold with equal preference. All such states have intensities comparable to that of the main line peak with those containing the same ionic core having similar intensities. These characteristics are noticeable in the lower resolution threshold spectrum of Hall *et al.* [11], and the trends of the two spectra are in agreement. More quantitative comparisons with their work are not possible due to a number of unresolved states within their spectrum and possible contributions from the decay of neutral resonances to lower lying ionic states, resulting in energetic electrons that are not fully discriminated against in threshold photoelectron spectroscopy employing static fields.

The trend from low to high photon energies, with the dominant correlations expected to change, can be clearly seen in Table I. All the observed satellites apart from two have a total angular momentum $J>1/2$, and so cannot be formed through FISCI with the parent $5s5p^6\ ^2S_{1/2}$ ionic state [25]. The formation of these satellites are expected to be due to continuum channel coupling and the calculations of Lagutin *et al.* [14] predict oscillations in $\beta(\omega)$ from 40 to 150 eV for these states due to the interference of several channels with different orbital momenta of the residual ion as well as of the photoelectron. The results at 40.8 and 63.5 eV are expected to be intermediate between the two extremes, where most states have not reached their high energy limits and others have already subsided in intensity from their threshold values. Indeed, by 72 eV, data presented by Lagutin *et al.* [14] show that the majority of states observed with binding energy 23–34 eV correspond to $J=1/2$ and $\beta\approx 2$, indicating a strong contribution from the $5s^{-1}$ main line. This becomes more extreme at still higher photon energies, and in the x-ray region states with $J=\frac{1}{2}$ are exclusively observed [12].

Calculations beyond the single-particle approximation in xenon that predict satellite positions and intensities are particularly challenging due to large relativistic effects and strong mixing between configurations. Pioneering calculations by Adam *et al.* [26] considered the formation of satellites due to FISCI in the high energy limit; these were expanded upon by Dyall and Larkins [27] and Hansen and Persson [15], and later treated on a relativistic footing by Kheifets and Amusia [28]. Tulkki [29] performed multichannel multi-configurational Dirac-Fock (MMCDF) calculations resulting in cross sections that start 4.31 eV above the 5s threshold for $J=\frac{1}{2}$ states. The CI-perturbation theory approach of Lagutin *et al.* [14] predicts the intensity of the $5s^25p^46s\ ^4P_{1/2}$ state to be $\approx$7% of the main line peak at their respective thresholds, and the cross sections for both states to vary with energy quite dramatically in this range, in contrast to the data of Samson and Gardner [20] for the $5s^{-1}$ state. We observe a relative intensity of 45% for the $^4P_{1/2}$ state relative to the main line peak, and it is our hope that the results presented here will initiate more quantitative studies in the low-energy region.

B. State-dependent lifetimes

In considering possible state-dependent decay or stabilization effects, it is noted that the lifetimes of Rydberg states are in general influenced both by core interactions (leading to the emission of radiation, autoionization, etc.) and external perturbations (such as collisional ionization and the lengthening of the lifetimes attributed to l and m mixing by electric fields and surrounding ions [30]). Within 4 cm^{-1} of an ionization limit the principal quantum number of a Rydberg electron is $\gtrsim$165 and the radiative lifetime for singly excited Rydberg states with these values of n is expected to be in the millisecond range [16], significantly longer than the maximum delay time between ionizing pulses in this experiment (3.24 μs). Within this waiting period, treating the Rydberg electron as a spectator and employing the electric dipole selection rules for parity that only even$\leftrightarrow$odd and for angular momentum that $\Delta J=0,\pm 1$, and the ionic cores with the exception of the $5s^25p^45d\ ^4D_{7/2}$, $5s^25p^45d\ ^4F_{9/2}$, and the $5s^25p^45d\ ^2F_{7/2}$ will fluoresce to the $5s^25p^5\ ^2P_{1/2,3/2}$ ionic states. These three states exhibit the shortest effective lifetimes of the observed states and suggest the core remains in an excited state for several microseconds, during which time there is an increased probability of autoionization, the result

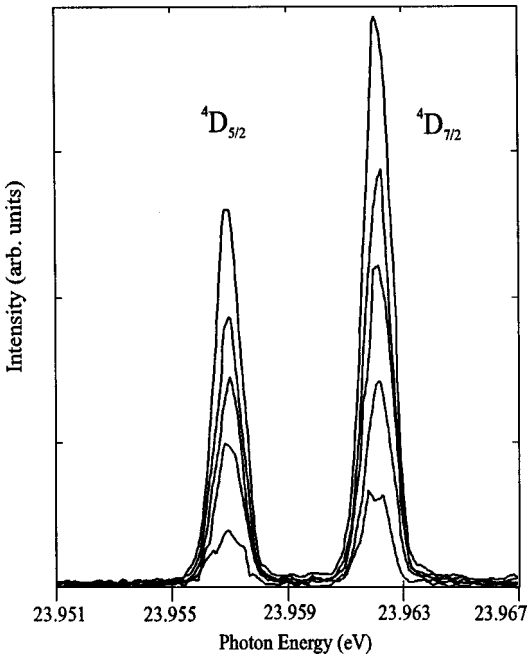

FIG. 4. The results of a pressure study on the observed $5s^25p(^3P)5d\ ^4D_{5/2}$ and $^4D_{7/2}$ intensities taken with the pulsed field applied every two ring periods. As the background pressure in the chamber was reduced through 1.4×10^{-5}, 1×10^{-5}, 7.4×10^{-6}, 4.8×10^{-6}, and 2.1×10^{-6} Torr, the intensities of both peaks decreased monotonically, with the ratio of the peaks remaining unchanged.

of which is observed as a decrease in Rydberg state population. It is unlikely that the emission of radiation due to an electric-dipole forbidden transition within these ionic cores perturbs their Rydberg electrons, causing an observable decay of Rydberg states, as fluorescence of the ionic core has been shown to have little effect in other species on the detection of high principal quantum number states [31]. Additionally we expect the other ionic cores to fluoresce, the only difference being a significantly shorter time scale. The effect of collisional ionization is expected to be largely independent of the particular state formed and in this experiment the density of background gas is the same at the thresholds for all ionic states. Studies on argon have demonstrated noticeable ion density effects, showing a decay of states with high n and a stabilization of states with low n for spectra taken at high ion densities relative to those obtained at lower densities [32]. The ion density in our experiment is approximately 200 cm^{-3}, lower by 10^5 than those investigated by Martin *et al.* [32]. To investigate any effect due to surrounding ions or Rydberg atoms, scans of the $5s^25p^45d\ ^4D_{5/2}$ and $^4D_{7/2}$ states were taken while varying the background pressure in the chamber over a factor of 5, with results shown in Fig. 4. The ratio of the observed signals for each state is essentially constant as the gas flow into the chamber is reduced, down to a background pressure as low as 2.1×10^{-6} Torr.

The effective lifetimes of the $5s5p^6$ $(^2S_{1/2})$ nl and all $5s^25p^46s$ $(^{2S+1}L_J)$ nl states are observed to be greater than 6 μs, in contrast to the majority of manifolds of Rydberg states that converge onto the $5s^25p^45d$ $(^{2S+1}L_J)$ core. With the exception of the $^4D_{5/2}$ state, all the remaining observed Rydberg states that are associated with this ionic core show effective lifetimes in the range from 0.8–4 μs. From Fig. 4 we conclude that these are insensitive to the background pressure in the chamber and the density of ions in the interaction volume, implying a selective *intra-atomic* phenomenon is being observed—that of an interaction between the Rydberg electron and the ionic core. Those states associated with a core of largest J exhibit the shortest lifetimes and the two states with $J=\frac{7}{2}$ show very similar values. It is not possible to conclusively deduce the exact mechanism behind the different decay rates observed, but a decrease in signal due to interaction of the Rydberg electron with an excited ionic core is generally consistent with the results. The $5s^25p^45d$ states are expected to have an outer electron which is on average more distant from the nucleus and therefore more likely to interact with the high-lying Rydberg electron, resulting in a loss of high Rydberg states through autoionization. In the meantime, the emission of radiation from the ionic core could be investigated by more extended fluorescence experiments at this energy range. Emision from the eight ionic states with electric dipole allowed transitions to the $5s^25p^5$ spin-orbit states within our energy range has been observed under discharge conditions [15] but more quantitative work remains to be done.

V. CONCLUSIONS

We have verified the positions and determined the relative intensities for formation of ten xenon correlation satellites formed at threshold 23.6–24.9 eV, both increasing the number of observed states from our previously published results [10] and obtaining effective lifetimes for the manifold of Rydberg states converging to each of these limits. The high-resolution technique of PFI-ZEKE photoelectron spectroscopy has allowed determination of the partial cross sections at threshold and provides a stringent test for the comparison of theoretical predictions. The effective lifetimes are seen to be independent of pressure but depend upon the quantum state of the ionic core, with five of the six manifolds of Rydberg states associated with the $5s^25p^45d$ core having a shorter lifetime than those converging onto the $5s^25p^46s$ core. Those cores with $J=\frac{5}{2}$ and $\frac{7}{2}$ are not allowed to relax by an electric dipole transition and exhibit the shortest lifetimes, suggesting an increased decay of Rydberg population through autoionization. We expect to extend these studies to other atomic systems, and to higher-lying satellite states, in the near future.

ACKNOWLEDGMENTS

This work was supported by the Natural Sciences and Engineering Research Council of Canada (NSERC), by the donors of the Petroleum Research Fund, administered by the American Chemical Society, and by the Office of Energy Research, Office of Basic Energy Sciences, Chemical Science Division of the U.S. Department of Energy. J.W.H. acknowledges the support of the Killam Foundation, M.E. acknowledges the support of GAANN and the Dow Chemical Corporation, and S.S. acknowledges the support of GAANN.

[1] *VUV and Soft X-Ray Photoionization*, edited by U. Becker and D. A. Shirley (Plenum, New York, 1996).
[2] K. Müller-Dethlefs and E. W. Schlag, Annu. Rev. Phys. Chem. **42**, 109 (1991).
[3] X. Zhang, J. M. Smith, and J. L. Knee, J. Chem. Phys. **99**, 3133 (1993).
[4] M. Evans, S. Stimson, C.-W. Hsu, and C. Y. Ng, J. Chem. Phys. **109**, 1285 (1998).
[5] J. W. Hepburn, in *Laser Techniques in Chemistry*, edited by A. B. Myers and T. R. Rizzo (Wiley, New York, 1995).
[6] H. Palm and F. Merkt, Appl. Phys. Lett. **73**, 157 (1998).
[7] F. Merkt and P. M. Guyon, J. Chem. Phys. **99**, 3400 (1993).
[8] B. Krässig, J. E. Hansen, W. Persson, and V. Schmidt, J. Phys. B **29**, L449 (1996).
[9] C.-W. Hsu, M. Evans, C. Y. Ng, and P. Heimann, Rev. Sci. Instrum. **68**, 1694 (1997); C.-W. Hsu, M. Evans, S. Stimson, C. Y. Ng, and P. Heimann, J. Chem. Phys. **106**, 8931 (1997).
[10] R. C. Shiell, M. Evans, S. Stimson, C.-W. Hsu, C. Y. Ng, and J. W. Hepburn, Phys. Rev. Lett. **80**, 472 (1998).
[11] R. I. Hall, L. Avaldi, G. Dawber, M. Zubek, and G. C. King, J. Phys. B **23**, 4469 (1990).
[12] S. Svensson, B. Eriksson, N. Mårtensson, G. Wendin, and U. Gelius, J. Electron Spectrosc. Relat. Phenom. **47**, 327 (1988).
[13] M. Carlsson-Göthe, P. Baltzer, and B. Wannberg, J. Phys. B **24**, 2477 (1991).
[14] B. M. Lagutin, I. D. Petrov, V. L. Sukhorukov, S. B. Whitfield, B. Langer, J. Viefhaus, R. Wehlitz, N. Berrah, W. Mahler, and U. Becker, J. Phys. B **29**, 937 (1996).
[15] J. E. Hansen and W. Persson, Phys. Scr. **36**, 602 (1987).
[16] *Rydberg States of Atoms and Molecules*, edited by R. F. Stebbings and F. B. Dunning (Cambridge University Press, Cambridge, 1983).
[17] C.-W. Hsu, M. Evans, S. Stimson, C. Y. Ng, and P. Heimann, Chem. Phys. **231**, 121 (1998).
[18] A. Kikas, S. J. Osbourne, A. Ausmees, S. Svensson, O.-P. Sairen, and S. Aksela, J. Electron Spectrosc. Relat. Phenom. **77**, 241 (1996).
[19] B. M. Lagutin, I. D. Petrov, V. L. Sukhorukov, S. B. Whitfield, B. Langer, N. Berrah, and U. Becker, J. Electron Spectrosc. Relat. Phenom. **76**, 337 (1995).
[20] J. A. R. Samson and J. L. Gardner, Phys. Rev. Lett. **33**, 671 (1974).
[21] H. Schmoranzer, S. Lauer, F. Vollweiler, G. Reichardt, K.-H. Schartner, G. Mentzel, O. Wilhelmi, V. L. Sukhorukov, B. M. Lagutin, and I. D. Petrov, Phys. Rev. Lett. **79**, 4546 (1997).
[22] U. Becker and D. A. Shirley, Phys. Scr. **T31**, 56 (1990).
[23] K. Codling and R. P. Madden, J. Res. Natl. Bur. Stand., Sect. A **76**, 1 (1972).
[24] R. I. Hall (private communication).
[25] S. B. Whitfield, B. Langer, J. Viefhaus, R. Wehlitz, N. Berrah, U. Becker, B. M. Lagutin, I. D. Petrov, and V. L. Sukhorukov, *Atomic and Molecular Photoionization*, edited by A. Yagishita and T. Sasaki (University Academic Press, Tokyo, Japan, 1996).
[26] M. Y. Adam, F. Wuilleimier, N. Sandner, V. Schmidt, and G. Wendin, J. Phys. (France) **39**, 129 (1978).
[27] K. G. Dyall and F. P. Larkins, J. Phys. B **15**, 219 (1982).
[28] A. S. Kheifets and M. Ya. Amusia, Phys. Rev. A **46**, 1261 (1992).
[29] J. Tulkki, Phys. Rev. Lett. **62**, 2817 (1989).
[30] W. A. Chupka, J. Chem. Phys. **98**, 4520 (1993).
[31] W. Kong, D. Rogers, and J. W. Hepburn, Chem. Phys. Lett. **221**, 301 (1994).
[32] J. D. D. Martin, C. Alcaraz, and J. W. Hepburn, J. Phys. Chem. **101**, 6728 (1997).